summing up the detonator, the plane-wave lens, and the HE-cylinder burn times. The difference can be partially attributed to the time necessary to shock the air adjacent to the HE. In order to simplify, in the following experimental and theoretical results presented here, the 80.6-µsec air shock initiation time will be taken as the new zero time reference for TOA data.

Figure 7 shows the experimental TOA data obtained from the light pipes and pressure transducers. The shock velocity, obtained by taking slopes of the TOA curve in Fig. 7, decreased from 1 cm/ μ sec near the HE to 0.2 cm/ μ sec at the end of the pipe. The time-interval meters indicated shock TOA of 0.467, 1.819, and 3.675 msec for the pressure transducers at 3, 9, and 15 m, respectively. These results are in good agreement with the scope records for these transducers.

A complete simulation of the venting associated with the HE region is not feasible. One limiting situation is no venting. The PUFL calculation which simulated no venting retained all of the HE gas and air from the HEMP calculations (shown in Fig. 5) within the boundaries shown in Fig. 4. The TOA results from this PUFL calculation, labeled P-1, included the effects of friction and heat transfer, and are shown (in Fig. 7) to agree favorably with the experimental TOA data.

One approximation for venting is that all of the HE with a negative velocity at 100 µsec after detonation

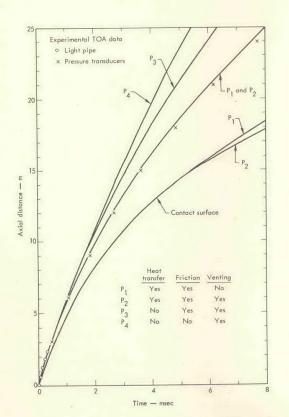
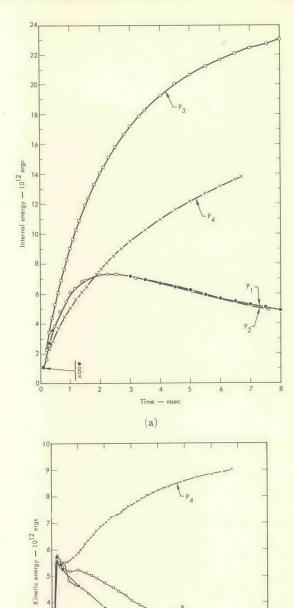


Fig. 7. Experimental and calculated shock position vs time.



(b)

Fig. 8. Results for driven air gas from PUFL; (a) internal energy versus time and (b) kinetic energy vs time.

vents—see Fig. 5(b). The PUFL calculations for venting omit all material with negative velocities in Fig. 5(b). Further, it can be conservatively approximated that starting at 100 μ sec after detonation, the left boundary of the material with positive velocities is exposed to atmospheric pressure. This approximation

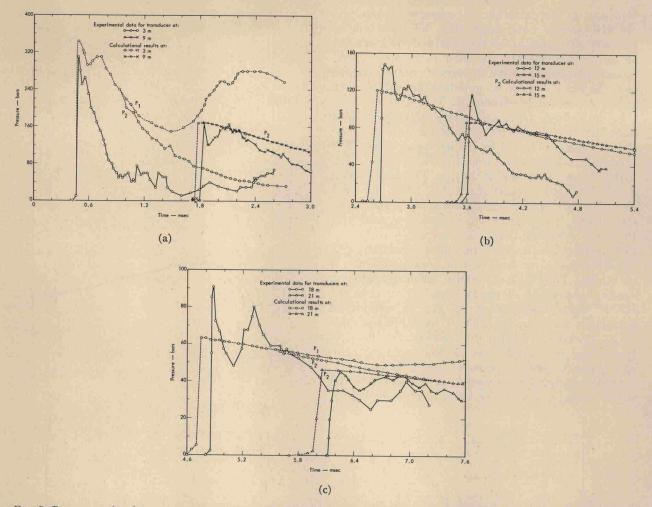


Fig. 9. Pressure vs time from pressure transducers and calculations at (a) 3 and 9 m, (b) 12 and 15 m, and (c) 18 and 21 m. Square denotes calculated arrival of contact surface.

is incorporated into the PUFL calculation by assigning one bar of pressure to the left boundary. The PUFL calculation P-2, for which these boundary approximations were used and in which and the effects of friction and heat transfer were considered, also gave very reasonable agreement with the TOA data (see Fig. 7).

The agreement in TOA results from these two PUFL calculations, in which venting and no venting were considered, indicates that the venting did not detectably affect the TOA data. Calculational results for the contact surface TOA's are given in Fig. 7 for the P-1 and P-2 cases. Rarefaction (from venting) does not appear to affect the motion of the contact surface for times less than 5 msec.

The P-1 and P-2 PUFL calculations considered the effects of convective heat transfer and friction. Preshot measurements in the exit pipe indicated an average "pipe radius-to-surface roughness" ratio of greater than 1000. Hence, the pipe was considered smooth, and a

dimensionless friction coefficient of $C_f/2=0.002$ was chosen¹² for the calculations. It is assumed that the Reynolds' analogy holds and that the Stanton number is also 0.002.

To investigate the relative effect of heat transfer and friction, two additional PUFL calculations, P-3 and P-4, were considered. In these calculations the same venting approximation as P-2 was used, and their TOA results are also shown in Fig. 7. In the P-4 calculation both heat transfer and friction were omitted. In the P-3 calculation heat transfer was omitted, but the effect of friction was considered. Figure 7 indicates that heat transfer significantly affects the TOA results.

In Figs. 8(a) and (b) the internal and kinetic energies in the air region are shown, respectively, as a function of time from the four calculations. In Fig. 8(a), the P-1 and P-2 calculations give nearly identical results out to 7 msec. This is further evidence that venting did not affect the time history of the shocked-air region.